Seismic Performance of Optimally Passive-Controlled Nonlinear Asymmetric Structures
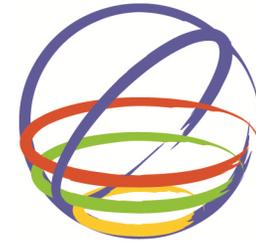
J.J. Aguirre, & J.L. Almazán
Pontificia Universidad Católica de Chile, Santiago, Chile.

15 WCEE
LISBOA 2012

SUMMARY:
Asymmetric structures are vulnerable to seismic excitation due to lateral-torsional coupling leading to uneven deformation demand among resisting planes. Enhance their structural performance by means of passive energy dissipation devices is an advisable solution. Nevertheless structural response is sensitive to the capacity and location of dampers. In order to overcome this issue the concept of torsional balance is applied through two methodologies: a formal optimization technique (Min-Max Algorithm) and a sequential procedure (Simplified Sequential Search Algorithm). Structural enhancement is valued via fragility curves which are developed through incremental dynamic analyses scaling an ensemble of 42 Chilean accelerograms recorded at the M_w 8.8 2010 Maule Earthquake. It is found that an optimal distribution of dampers achieves torsional balance. Asymmetric structures optimally passive-controlled can be classified as symmetric even attaining a structural performance increment. However fragility curves denote that special care should be taken when reducing the strength of the structure.

Keywords: Torsional balance, energy dissipation, fragility analysis.

1. INTRODUCTION

Traditional earthquake resistant design relies on the capacity of structures to sustain inelastic incursions when subjected to a design-level seismic ground motion while avoiding catastrophic failures and loss of life. Asymmetric structures are particularly vulnerable to seismic action due to torsional response which implies concentration of deformation in some resisting planes focusing damage in few elements.

An advisable solution to mitigate the harmful torsional response of structures is through the use of supplemental Energy Dissipation Devices (EDD). The planwise distribution of EDD has an important influence in the response of asymmetric-plan structures as denoted by studies conducted through parametric, single-story systems (Goel 1998, 2001, Lin and Chopra 2003), therefore an appropriate selection of EDD capacities and locations is required.

The allocation of EDD has been conducted through different optimization schemes. A sequential optimization procedure was initially developed by Zhang and Soong (1992). A simplified version of that algorithm was letter proposed by López-García (2001, 2002) called the Simplified Sequential Search Algorithm. Lavan and Levy (2005, 2006a, 2006b, 2006c) have developed formal optimization algorithms that introduce Performance Indexes (PI) as a constraint function.

The concept of torsional balance has been proposed as a design methodology for asymmetric structures with EDD (Almazán and De la Llera 2009, De la Llera et al. 2005, García et al. 2007). It is defined as the property of an asymmetric structure with equal deformation demand in structural members equidistant from the Geometric Center (GC). It implies minimizing lateral-torsional coupling.

In this context, it turns out important to study procedures to efficiently distribute EDD in plan as well as height. The Min-Max Algorithm is presented as an optimization technique and it is compared with a simple, practical and straight forward algorithm such as the SSSA considering the linear and nonlinear

behaviour of the structures. Later, the optimal damping distribution obtained via SSSA is valued through a damage assessment via a probabilistic procedure known as the Incremental Dynamic Analysis (IDA) (Vamvatsikos and Cornell 2002, Vamvatsilos and Fragiadakis 2009). It consists in performing nonlinear time-history dynamic analysis for an ensemble of earthquake ground motions scaled to represent a specific intensity. It allows tracking the complete range of structural behaviour, from elastic response to yielding and finally collapse.

2. STRUCTURAL SYSTEMS

Two structural models are considered in this research (Fig. 1). Model M1 is a two-story plane frame with natural frequency $\omega=2\pi$. The second model is a parametric, monosymmetric, single-story system with a 1:3 plan aspect ratio. It consists of four resisting planes in the Y-direction and two in the X-direction. Two cases are considered: a torsionally-stiff model (M2$_a$) with a frequency ratio $\Omega_s=\omega_\theta/\omega_y=1.33$ and a torsionally-flexible model (M2$_b$) $\Omega_s=0.75$. Asymmetry is induced by shifting the Center of Mass (CM) an amount e_s away from the Center of Stiffness (CS) along the X-axis.
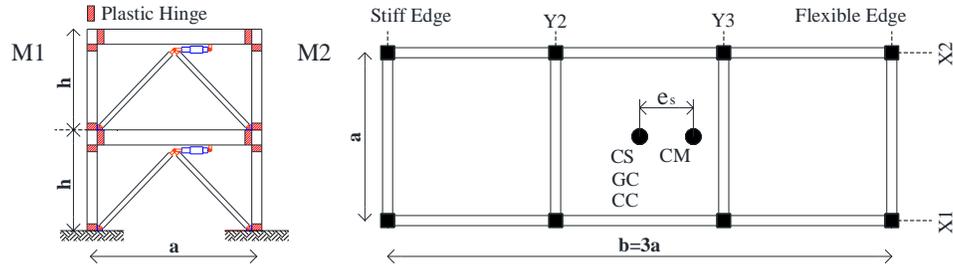
Figure 1. Models M1 and M2 considered in this research

2.1. Nonlinear analysis

The inelastic response of both structures is considered through the well-known Bouc-Wen model (Bouc 1971, Wen 1976). Model M1 is implemented with bilinear flexural hinges at the extreme of beams and columns. Due to the parametric nature of Model M2, the nonlinear constitutive behaviour of each resisting plane is calibrated to match the static nonlinear push-over curve of model M1. A trilinear curve is adjusted by adding two Bouc-Wen models.

3. OPTIMIZATION ALGORITHMS

Structural response is computed through time-history analyses. The reference excitation is a synthetic accelerogram compatible with the design spectrum of the seismic isolation Chilean code (NCh-2745, 2003) for firm soil.

3.1. The Min-Max Algorithm

an optimization algorithm called Min-Max Algorithm (MMA) is formulated according to the torsional balance criterion. The objective function J is the performance index subjected to a total added damping constraint. The optimization scheme for the general case that considers nonlinear dampers and the inelastic response of the main structure is expressed as:

$$\text{Minimize: } J = \max_j\left(\|PI_j\|\right) \tag{1}$$

$$\text{Subject to:} \begin{cases} M\ddot{q} + C\dot{q} + Kq + L_p{}^T f_p(\delta_p, \dot{\delta}_p, z_p) = -MR\ddot{u}_g - L_s{}^T f_s(\delta_s, \dot{\delta}_s, z_s) \\ \dot{z}_p = \dot{z}_p(\delta_p, \dot{\delta}_p, z_p) \\ \dot{z}_p = \dot{z}_p(\delta_s, \dot{\delta}_s, z_s) \\ \delta_p = L_p q \\ \delta_s = L_s q \\ f_p = f_p(\delta_p, \dot{\delta}_p, z_p) \\ f_s = \zeta \hat{f}_s(\delta_s, \dot{\delta}_s, z_s) \\ \zeta = \text{diag}(\zeta_1, \zeta_2, \dots \zeta_m) \\ \Sigma_{i=1}^m \zeta_i \le \zeta_{tot} \\ \zeta_i \ge 0 \end{cases}$$

where J is $PI_j = \max_t(||\delta_{s_j}(t)||)$; M, K, C are the mass, stiffness and damping structural matrices; q is the structure degrees of freedom vector; f_s, δ_s, z_s are the force, deformation and the hysteretic variable vectors associated to the EDD; f_p, δ_p, z_p are the force, deformation and the hysteretic variable vectors associated to the inelastic behaviour of the main structure; L_p, L_s are kinematic transformation matrices; ζ is a diagonal matrix with the capacities of the EDD, being $\hat{f}_s$ a unit capacity vector force and ζ_{tot} is the total added damping capacity to be spatially distributed in the structure; $\ddot{u}_g$ is the ground acceleration vector and R its q-DOF allocation vector.

3.2. The Simplified Sequential Search Algorithm

In order to propose an optimization scheme feasible to be implemented by practicing engineers, the SSSA is compared with the MMA, a formal optimization technique that requires a sophisticated algorithm. The SSSA, as its name denotes, is a sequential procedure where a predefined damping capacity is placed sequentially where de location of the PI is maximum. The structure is updated at each step and the analysis is repeated up to the performance objective is achieved or the total damping capacity is distributed.

3.3. Seismic Performance Assessment

The seismic enhancement of structures M1 and M2 equipped with an optimal distribution of EDD is evaluated through fragility analysis considering a different approach for each structure. For structure M1, the Performance-Based seismic Design (PBD) framework is considered (PEER, 2008). Fragility curves, which basically denote the conditional probability of exceeding a limit state, are developed through IDA. The horizontal components of the 21 accelerograms recorded at the Mw 8.8 2010 Maule Earthquake are considered. Each accelerogram is scaled to twelve intensities, among them, the PBD predefined hazard levels named: very frequent (with a return period T_R=43 years, frequent (T_R=72 years), design (T_R=475 years) and maximum credible earthquake (T_R=950 years). According to FEMA 376 guidelines (2000), four limit states are verified through a drift limit: Operational (OP), Immediate Occupancy (IO), Life Safety (LS) and Collapse Prevention (CP).

Due to the parametric nature of model M2, structural performance is assessed as function of damage reduction. Structural damage depends not only on the maximum deformation (drift) that a structure experiences when subjected to an earthquake loading, but in the hysteretic energy (cycles of loading and unloading) that is dissipated through the event (Park and Ang 1985a, 1985b). In this way, damage is assessed through an empirical measure such as the Park & Ang index. This Damage Index (DI) is composed of two main parameters, the first related with the damage caused by the deformation and the second related to the structural hysteretic dissipated energy.

$$DI = \frac{x_{max}}{x_u} + \beta \frac{E_H}{F_y x_u} \tag{2}$$

where x_{max} is the maximum deformation of the structure; x_u is the ultimate deformation capacity under static loading; E_H is the cumulative absorbed hysteretic energy; F_y is the yield strength and β is a coefficient for cyclic loading effect whose value depends on specific structural characteristics. A structure with DI < 0.2 may be considered to have slight damage, DI < 0.4 represents moderate damage and DI > 0.4 represents damage beyond repair. While DI = 1.0 means total damage or complete collapse. Let us recall that the basic principle of conventional earthquake-resistant design implies that a structure should not collapse when subjected to a design-level seismic ground motion, and the occupants can evacuate it safely. The structure has fulfilled its function even though it may never be functional again (Christopoulos and Filiatrault 2006). Under this premises, factor β is calibrated to get a DI=0.40 when the symmetric structure is subjected to a reference synthetic accelerogram compatible with the Chilean design spectrum. This assumption implies greater damage for asymmetric structures. The ultimate deformation capacity of the structure is defined as $x_u = 4x_y$, where x_y is defined as the deformation limit where instability begins (FEMA 356, 2000).

4. ANALYSES AND RESULTS

The MMA and the SSSA are implemented and compared for the linear and nonlinear M1 and M2 structures. For the sake of simplicity, only linear viscous dampers are considered at this stage. Drift is defined as the performance index.

4.1. Optimal damping distribution of M1 and M2 models.

Fig. 2 shows the contour lines of the Maximum Drift Deformation (MDD) normalized to the MDD of the bare structure versus added damping quantities c_1 and c_2 installed respectively at the first and second story of structure M1. The left graphic represents the linear structure while the left one considers the inelastic response of the main structure. Added damping quantities are normalized to a reference quantity c_{reff} which supplies an additional 15% damping ratio in the principal vibration mode. The reference quantity assumes a uniform height distribution. The solid red is the MMA solution; it represents the optimal combination of capacities c_1 and c_2 that minimizes the MMD. Balance is attained when the added damping capacity installed at the first story is greater than c_{reff}. The SSSA is represented by the staggered black line for a 10% discrete added damping quantity ($c_{reff}/10$) at each step. The SSSA solution converges to the MMA solution as step increments are further reduced. Damping quantities distribution of the nonlinear model are similar to the linear one, on the other hand, MMD reductions quantified by the linear model are slightly larger than reductions obtained by the nonlinear analysis.
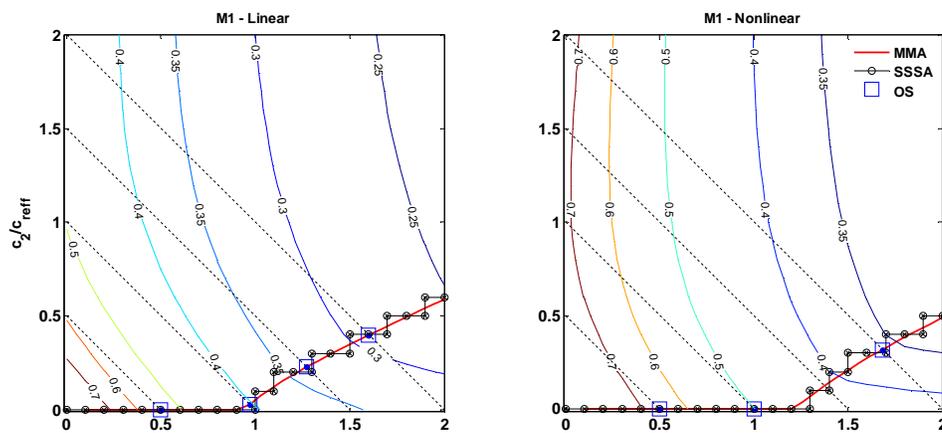
Figure 2. Linear and nonlinear model M1 contour lines of the normalized drift reduction. MMA and SSSA solution comparison

The last analysis is repeated for structures M2a and M2b. Fig. 3 and 4 show the contour lines of the MDD as function of normalized added damping quantities c_1 and c_2 installed at the flexible and stiff edges respectively. The reference added damping quantity assumes the uniform plan distribution that brings an additional 15% damping ratio in the mode with the greater modal participation factor. The solid red line represents the quantities c_1 and c_2 combination that achieve torsional balance (De la Llera et al. 2005). As before, the SSSA discrete solution is represented by the staggered black line for a 10% discrete added damping quantity ($c_{reff}/10$) at each step.
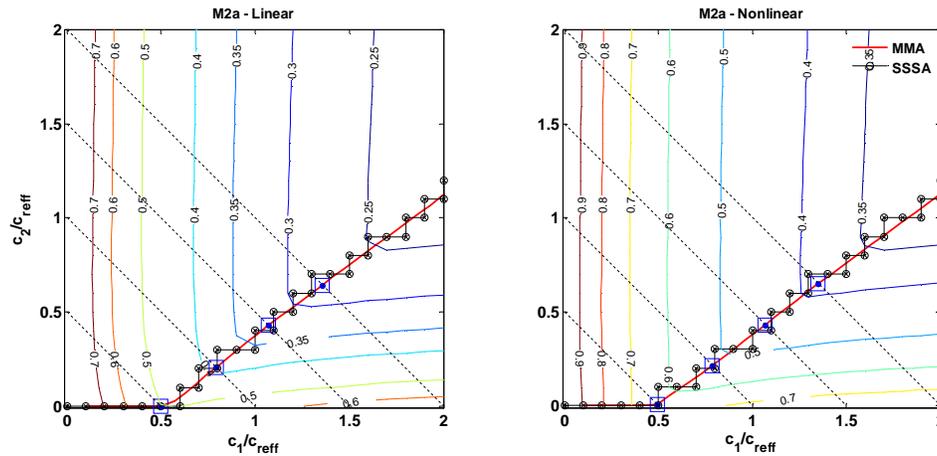
Figure 3. Linear and nonlinear model M2a (torsionally-stiff) contour lines of the normalized drift reduction. MMA and SSSA solution comparison.
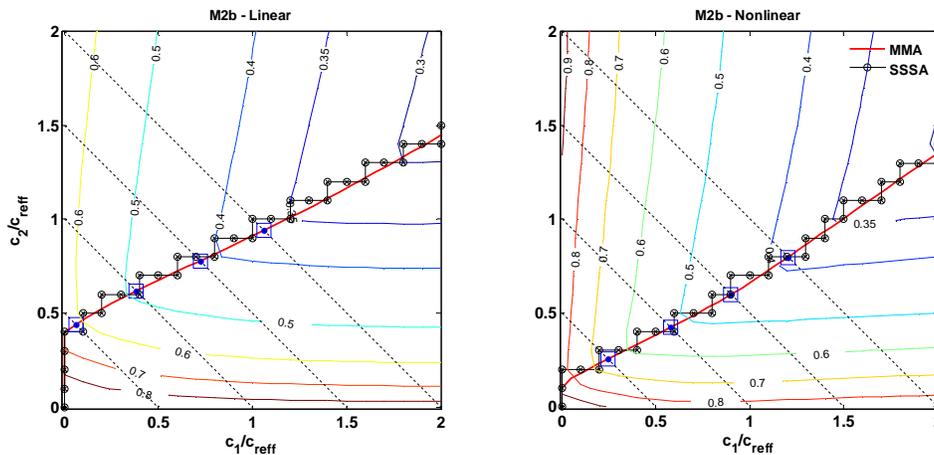
Figure 4. Linear and nonlinear model M2a (torsionally-stiff) contour lines of the normalized drift reduction. MMA and SSSA solution comparison.

Torsionally-stiff structures experience larger deformations at the flexible edge therefore this edge requires larger c_1 damping capacities. On the other hand, torsionally-flexible structures undergo larger demands at the stiff edge, consequently damping quantities c_1 are smaller than c_2. The same observations of model M1 apply to the comparison between the linear and the nonlinear analysis of model M2: damping quantities distributions are similar and deformation reductions are slightly overestimated by the linear analysis.

These analyses unveil that the SSSA solution is the discrete solution of the MMA and both are optimal solutions of plan and height damping distribution. The linear analyses can adequately approximate the nonlinear damping distribution solution.

4.2. Seismic Performance and Damage Reduction
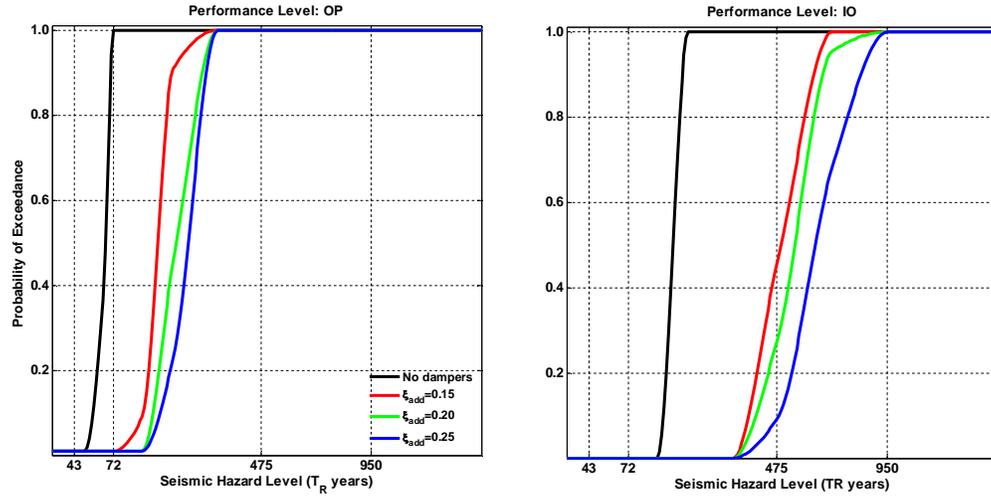
Figure 5. Model M1 fragility curves for OP and IO performance levels.
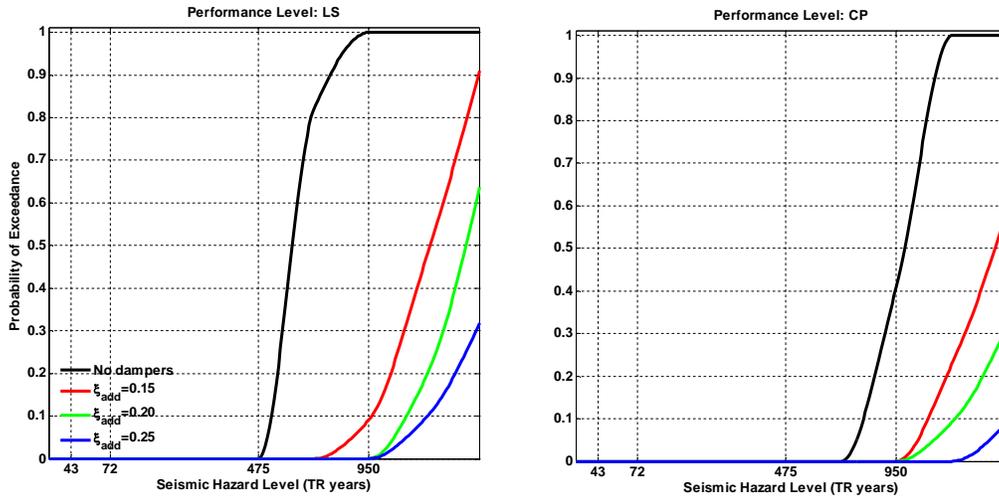
Figure 6. Model M1 fragility curves for LS and CP performance levels.

According to the previous subsection, structures M1 and M2 are equipped with the optimal damping distribution that linear analyses bring and their performance enhancement is assessed through fragility analysis. Fig. 5 and Fig. 6 show the fragility curves of structure M1. Four cases are considered: the bare structure (no dampers), and three levels of added damping: $\xi_{add} = 0.15, 0.20, 0.25$. Four limit states are verified: OP, IO, LS and CP. The capacity of the structure is assigned according to the Chilean seismic code NCh-433 (1996), thus a response modification factor R=7 is considered. Structures can be classified into three categories according to the expected seismic performance level: basic (B), essential (E) and critical (C) according to FEMA 356 (2000) and should verify the performance objectives according to Table 1. The OP performance level is verified by the basic structure. An essential structure requires seismic enhancement to verify this performance objective, but the critical facility is unable to develop it. A similar observation can be made to the IO limit state. The basic structure verifies the LS performance level, but the essential structure requires additional damping. The last performance verification, CP is partially fulfilled by the bare basic structure, but if dampers are added the performance objective fully is achieved

Table 1. Seismic Performance Objectives for buildings

	Performance Level			
Hazard	OP	IO	LS	CP
43	B	-	-	-
72	E	B	-	-
475	C	E	B	-
950	-	C	E	B

Fig. 7, 8 and 9 show the damage curves of structure M2. Four cases are considered as before: the bare structure (no dampers), and three levels of added damping: $\xi_{add} = 0.15, 0.20, 0.25$. Three capacities are studied: (i) the structure with the full capacity as defined in subsection 3.3, denoted as F_y=1.00 (ii) the structure with a 25% capacity reduction: F_y=0.75, and (iii) the structure with a 40% capacity reduction: F_y=0.60. Results are shown for the torsionally-flexible model (M2b) due to it represents the most vulnerable structural condition. Curves of the stiff (SE) and flexible edges (FE) are plotted separately to appreciate the balance of the structure when achieved.

The FE is the edge with the highest drift demand, therefore optimization algorithms add damping at this edge up to drift at both edges is equalized (torsional balance is achieved). Before balance is achieved, deformations at the stiff edge may increase, which implies that for small amounts of added damping damage at the stiff edge may increase too. This observation, appreciated for the structure with a fundamental period of $T \geq 2.0s$, should be considered as a reduction and spread of previous damage concentrations. On the other hand, the FE shows a monotonically damage reduction when dampers are added.

As mentioned before, the asymmetric structure is predefined to experience greater damage than the symmetric structure. It implies DI>0.40 for the design intensity (T_R=475years). But when sufficient damping is added according to the optimal design criterion, performance of the asymmetric structure is enhanced beyond performance of the symmetric counterpart. This observation is valid only when the structure does not have any capacity reduction. The analysis with a 25% capacity reduction and 25% of added damping is the only case studied that the asymmetric structure equalizes performance of the symmetric one.
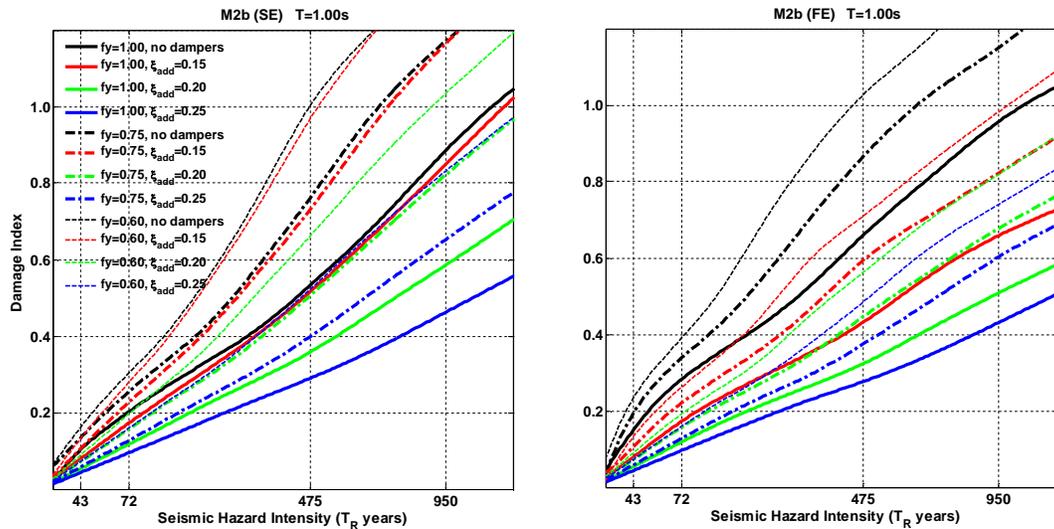
Figure 7. Model M2b stiff (left) and flexible (right) edges damage curves. T=1.00s.
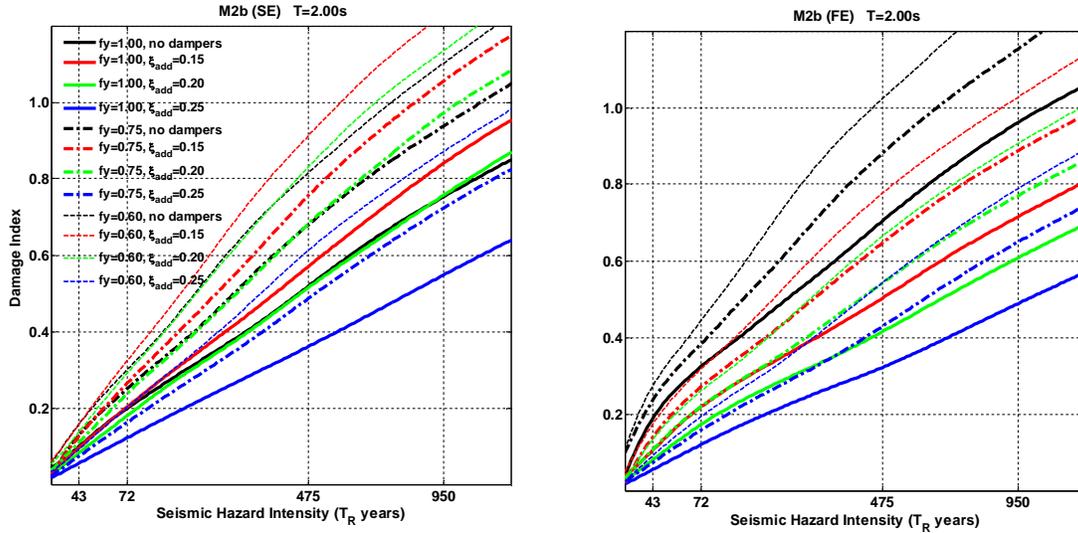
Figure 8. Model M2b stiff (left) and flexible (right) edges damage curves. T=2.00s.
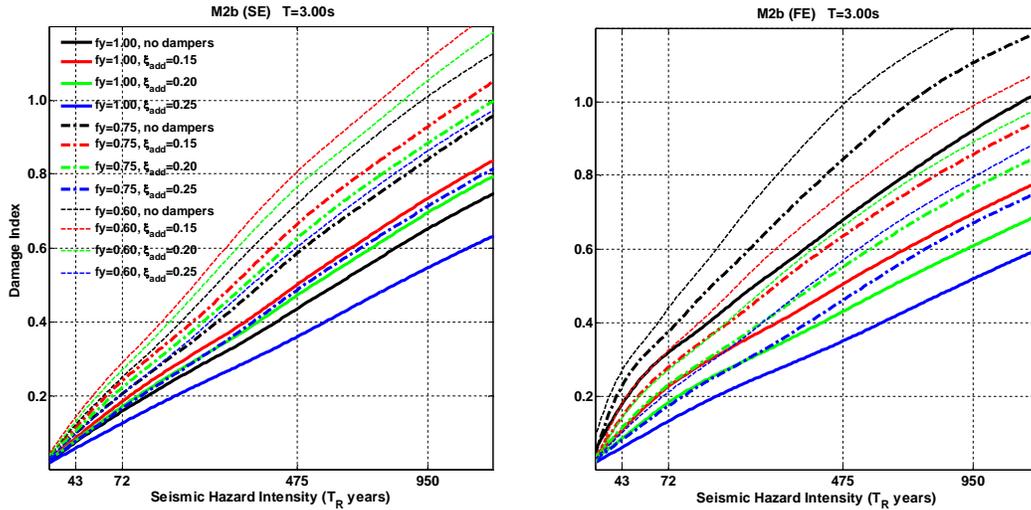
Figure 9. Model M2b stiff (left) and flexible (right) edges damage curves. T=3.00s.

These observations are more evident at Fig. 10 which shows the monotonic damage reduction of model M2b flexible edge as dampers are added as function of the fundamental period of the structure.

5. CONCLUSIONS

The Min-Max Algorithm is presented as an optimization technique to find the optimal height and plan distribution of dampers according to a performance index. The models considered in this research show that a simple methodology such as the Simplified Sequential Search Algorithm is found to be a discrete approximation that converges to the MMA exact solution as added damping increments are reduced. Linear models can adequately approximate the optimal damping distribution when considering the inelastic response of the structure.
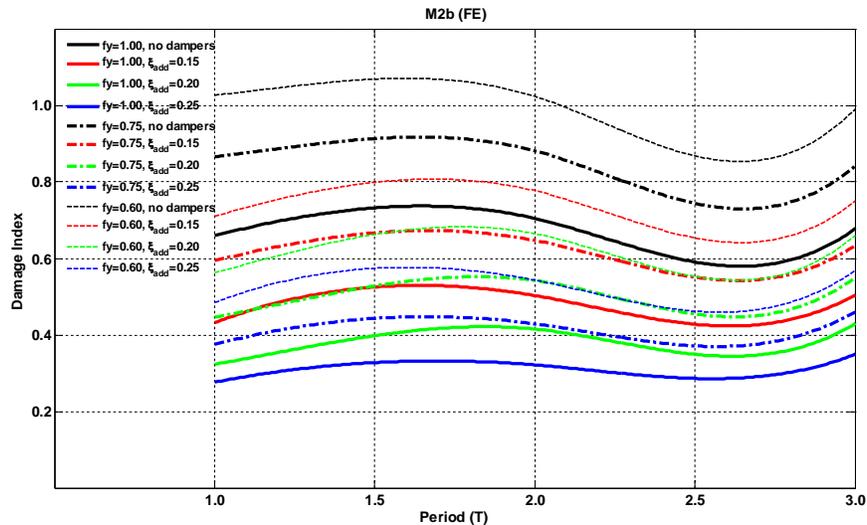
Figure 10. Model M2b-FE damage reduction as function of the fundamental period of the structure.

Then, the performance of the optimally passive-controlled is assesses through fragility and damage curves. Model M1 fragility curves denote that a basic-categorized structure accomplishes the expected performance objective for all limit states. An essential-categorized structure requires additional damping to fulfill its performance objective, but a critical facility requires not only additional damping but also additional strength.

Model M2 damage analysis show that asymmetric structures can be balanced in terms of deformation and damage. Their performance can be raised beyond the symmetric counterpart, thus asymmetric structures optimally passive-controlled may be classified as symmetric.

Strength plays an important role into the performance of the structures. Strength reduction should be carefully implemented in order to assure a reasonable performance enhancement which is the aim of seismic protection systems.

REFERENCES

Almazán, J.L., De la Llera, J.C. (2009). Torsional balance as new design criterion for asymmetric structures with energy dissipation devices. *Earthquake Engineering and Structural Dynamics*. **38:** 1421-1440.
Aguirre, J.J. (to be published). Seismic design of optimally-passive controlled nonlinear asymmetric structures. A performance based design approach. PhD. dissertation. Pontificia Universidad Católica de Chile.
Bouc, R. (1971). Modèle mathématique d'hystérésis. Acustica. **21:** 16-25
Christopoulos, C. and Filiatrault, A. (2006): Principles of Passive Supplemental Damping and Seismic Isolation. IUSS Press, Pavia-Itlay.
De la Llera, J.C., Almazán, J.L. and Vial, I.J. (2005). Torsional balance of plan-asymmetric structures with frictional dampers: analytical results. *Earthquake Engineering and Structural Dynamics*. **34:** 1089-1108.
Fema 356. (2000). Prestandard and commentary for the seismic rehabilitation of buildings. ASCE American Society of Civil Engineers.
García, M., De la Llera, J.C. and Almazán, J.L. (2007). Torsional balance of plan asymmetric structures with viscoelastic dampers. Engineering Structures. **29:** 914-932.

Goel, R.K. (1998). Effects of supplemental viscous damping on seismic response of asymmetric-plan systems. *Earthquake Engineering and Structural Dynamics*. **27:** 125-141.

Goel, R.K. and Booker, C.A. (2001). Effects of supplemental viscous damping on inelastic seismic response of asymmetric systems. *Earthquake Engineering and Structural Dynamics*. **30:** 411-430.

Lavan, O. and Levy, R. (2005). Optimal design of supplemental viscous dampers for irregular shear-frames in the presence of yielding. *Earthquake Engineering and Structural Dynamics*. **34:** 889-907.

Lavan, O. and Levy, R. (2006). Optimal design of supplemental viscous dampers for linear framed structures. *Earthquake Engineering and Structural Dynamics*. **35:** 337-356.

Lavan, O. and Levy, R. (2006). Optimal peripheral drift control of 3D irregular framed structures using supplemental viscous dampers. *Journal of Earthquake Engineering*. **10:6**, 903-923.

Levy, R. and Lavan, O. (2006). Fully stressed design of passive controllers in framed structures for seismic loadings. *Structural Multidisciplinary Optimization*. **32:** 485-498.

Lin, W.H. and Chopra, A.K. (2003). Asymmetric one-storey elastic systems with non-linear viscous and viscoelastic dampers: earthquake response. *Earthquake Engineering and Structural Dynamics*. **32:** 555-577.

López-García, D. (2001). A simple method for the design of optimal damper configurations in MDOF structures. *Earthquake Spectra*. **17:3**, 387-398.

López-García, D., and Soong, T.T. (2002). Efficiency of a simple approach to damper allocation in MDOF structures. *Journal of Structural Control*. **9:** 19-30.

NCh-433. (1996). Diseño sísmico de edificios. Instituto Nacional de Normalización. Santiago, Chile.

NCh-2745. (2003). Análisis y Diseño de edificios con aislación sísmica. Instituto Nacional de Normalización. Santiago, Chile.

Park, Y.J. and Ang, A. (1985). Mechanistic Seismic Damage Model for Reinforced Concrete. *Journal of Structural Engineering*. 111:4, 722-739.

Park, Y.J., Ang, A., and Wen, Y.K. (1985). Seismic Damage Analysis of Reinforced Concrete Buildings. *Journal of Structural Engineering*. 111:4, 740-757.

PEER Report. (2008). An Assessment to Benchmark the Seismic Performance of a Code-Conforming Reinforced Concrete Moment-Frame Building. Pacific Earthquake Engineering Research Center.

Vamvatsikos, D. and Cornell, C. A. (2002). Incremental Dynamic Analysis. *Earthquake Engineering and Structural Dynamics*. **31:** 491-514.

Vamvatsikos, D. and Fragiadakis, M. (2009). Incremental dynamic analysis for estimating seismic performance sensitivity and uncertainty. *Earthquake Engineering and Structural Dynamics*. **39:** 141-163.

Wen, Y.K. (1976). Method for random vibration of hysteretic systems. *Journal of the Engineering Mechanics Division*. **102:** 246-263.

Zhang RH, Soong TT. 1992. Seismic design of viscoelastic dampers for structural applications. *Journal of Structural Engineering*. **118:5**, 1375-1392 .